



CuCrO₂ Delafossite: A Stable Copper Catalyst for Chlorine Production**

Amol P. Amrute, Gastón O. Larrazábal, Cecilia Mondelli, and Javier Pérez-Ramírez*

Around 1870, Henry Deacon discovered a process to valorize the large amounts of gaseous HCl, originating as a by-product of the Leblanc process, by catalytic oxidation to Cl₂,^[1] which was used to make bleaching powder. Employing a pumice-supported CuCl₂ catalyst in a fixed-bed reactor, the Deacon process constituted the first large-scale application of heterogeneous catalysis and one of the first examples in industry of the “waste-to-product” approach.^[2] This process did not last long in industry because the Leblanc process for Na₂CO₃ production was superseded by the less wasteful Solvay process, and with the development of suitable generators at the end of the 19th century, Cl₂ was exclusively manufactured by NaCl electrolysis. The story now repeats itself, 140 years after Deacon. Currently, the recycling of by-product HCl from phosgenation processes (e.g. polyurethane and polycarbonates production) by conversion to Cl₂ is in high demand.^[1] However, neither the original Deacon catalyst, nor the multitude of (promoted) Cu-based systems developed during the 20th century offer a feasible solution, because they deactivate rapidly owing to the volatilization of copper chlorides under the reaction conditions.^[2,3] Any copper-based catalyst reported to date suffers from fast bulk chlorination, leading to volatile CuCl₂ and CuCl, which translate into short catalyst lifetimes and severe corrosion issues in the plant.^[3]

Owing to these constraints, contemporary efforts focused on RuO₂-based catalysts, which preserve their bulk structure in HCl oxidation, leading to stable Cl₂ production in pilot trials and plant installations.^[4] Despite this success, the development of industrial catalysts based on copper is highly appealing owing to the much lower price of copper compared to ruthenium. Our efforts in this direction resulted in CuAlO₂,^[5] which showed stable Cl₂ production during 1000 hours on stream but (as usual) experienced critical bulk changes and a significant copper loss of 40 % at the end of the run. Further efforts around the delafossite structure have ended with the discovery of CuCrO₂ as the first Cu-based catalyst displaying a high activity for HCl oxidation while

preserving its bulk structure under reaction conditions. Herein, we show the unique stability of CuCrO₂ under chlorinating and oxidizing environments, which is vital to guarantee its durability. Building on this result, a novel CuCrO₂-CeO₂ composite for HCl oxidation is presented, with a fourfold activity increase compared to the pure CuCrO₂ and CeO₂ phases. This catalytic system enables a cost-effective and energy-efficient technology for Cl₂ production.

The structure of cuprous delafossites (CuMO₂) can be visualized as the stacking of planer layers of Cu⁺ cations and layers of edge-sharing M³⁺O₆ octahedra (Figure 1).^[6] Typical

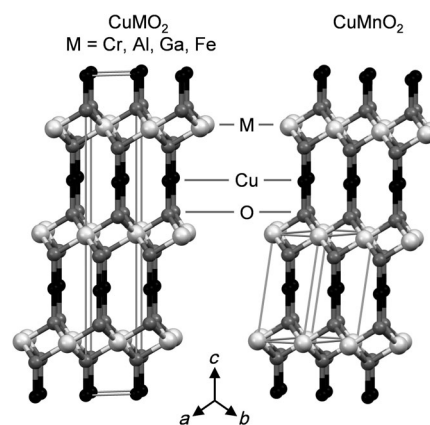


Figure 1. Rhombohedral structure of delafossite common to CuCrO₂, CuAlO₂, CuGaO₂, and CuFeO₂ (left) and the distorted CuMnO₂ with a monoclinic structure (right).

M³⁺ cations include Al, Cr, Fe, Co, Ga, Y, In, La, Nd, and Eu.^[7] CuCrO₂ and CuAlO₂ have received considerable attention as transparent conducting oxides for optoelectronic device technology.^[8] However, their use in catalysis is scarce, with reported applications in methanol synthesis, N₂O decomposition, methanol steam reforming, and photocatalytic H₂ evolution and NO₃⁻ removal.^[9]

Single-phase cuprous delafossites were synthesized by the solid-state reaction of an equimolar mixture of Cu₂O and M₂O₃ (M = Cr, Al, Ga, Fe, Mn) at 1273–1423 K for 30 hours. As shown in Figure 2 a, the X-ray diffraction (XRD) patterns of CuCrO₂, CuAlO₂, CuGaO₂, and CuFeO₂ match the characteristic rhombohedral structure (space group *R*3̄*m*), while that of CuMnO₂ corresponds to the monoclinic structure (space group *C*2/*m*).^[6,10] The anomaly of CuMnO₂ (known as crednerite) is related to the Jahn–Teller distortion, which leads to a large difference between apical and equatorial Mn–O distances within the Mn³⁺O₆ octahedra.^[11]

[*] A. P. Amrute, G. O. Larrazábal, Dr. C. Mondelli, Prof. J. Pérez-Ramírez
Institute for Chemical and Bioengineering, Department of Chemistry and Applied Biosciences, ETH Zurich
Wolfgang-Pauli-Strasse 10, 8093 Zurich (Switzerland)
E-mail: jpr@chem.ethz.ch

[**] Bayer MaterialScience AG is acknowledged for permission to publish these results. Dr. Z. Łodziana is thanked for providing the thermodynamic data.

Supporting information for this article is available on the WWW under <http://dx.doi.org/10.1002/ange.201304254>.

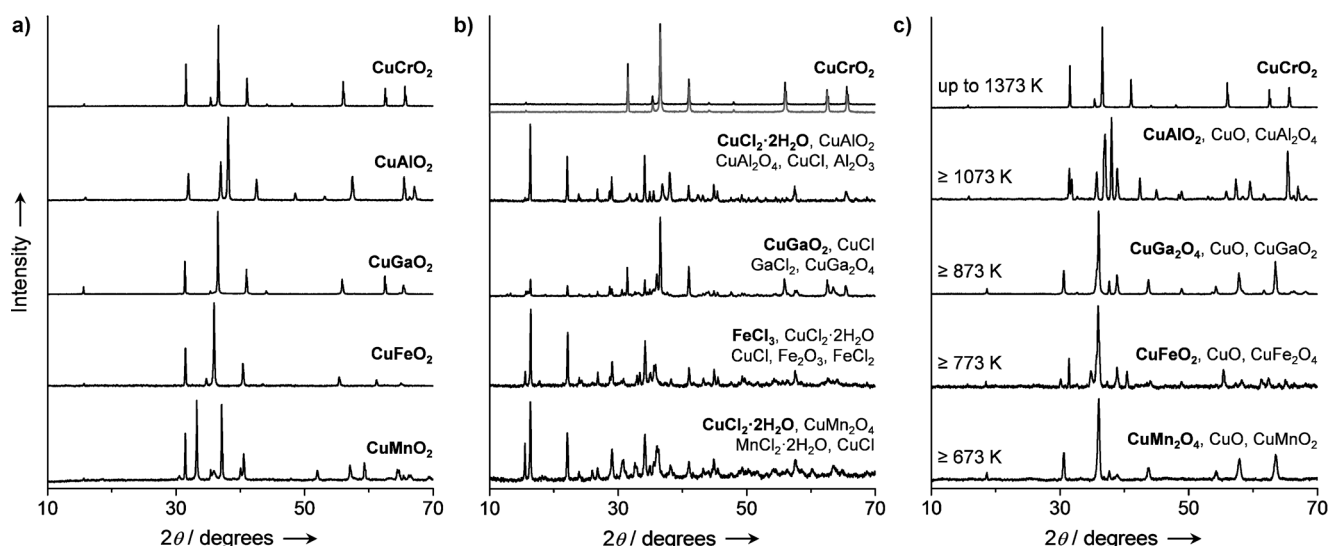


Figure 2. X-ray diffraction patterns of the a) as-prepared cuprous delafossites, b) after HCl oxidation at 573–690 K, and c) after treatment at various temperatures in air. The gray pattern in the top section of (b) corresponds to the CuCrO_2 sample treated in pure HCl at 690 K. The crystalline phases identified in the samples are listed on the right of the patterns, with the predominant component in bold.

Catalytic tests of HCl oxidation (Figure 3a) revealed that CuCrO_2 was the most active delafossite, closely followed by CuAlO_2 , while CuMnO_2 and CuGaO_2 exhibited inferior activity. The run over CuFeO_2 was interrupted at 630 K owing to significant metal loss in the form of volatile FeCl_3 (boiling point of 588 K). The apparent activation energy estimated for CuCrO_2 and CuAlO_2 was approximately 90 kJ mol^{-1} and 140 kJ mol^{-1} for CuGaO_2 and CuMnO_2 . However, the most exciting results were obtained by XRD analysis of the post-reacting samples. The structure of CuCrO_2 was unchanged in HCl oxidation at 573–690 K and even in pure HCl (i.e. without gas-phase O_2) at 690 K for ten hours (Figure 2b). Contrarily, CuAlO_2 , CuGaO_2 , CuFeO_2 , and CuMnO_2 exhibited prominent bulk changes under HCl oxidation for five hours with the identification of metal chlorides ($\text{CuCl}_2 \cdot 2\text{H}_2\text{O}$, CuCl , GaCl_2 , FeCl_3 , FeCl_2 , $\text{MnCl}_2 \cdot 2\text{H}_2\text{O}$) and spinels (CuAl_2O_4 , CuGa_2O_4 , CuMn_2O_4). These bulk changes are related to the fact that Cu^+ in the delafossite structure is prone to oxidation, eventually leading to phase transformations ($2\text{CuMO}_2 + \frac{1}{2}\text{O}_2 \rightarrow \text{CuO} + \text{CuM}_2\text{O}_4$ and $\text{CuM}_2\text{O}_4 \rightarrow$

$\text{CuO} + \text{M}_2\text{O}_3$) and instantaneous chlorination of the resulting single oxides. This was supported by XRD analysis of the delafossites treated in air at various temperatures for five hours (Figure 2c). CuCrO_2 was stable at all temperatures up to its synthesis temperature (1373 K). In contrast, CuMnO_2 , CuFeO_2 , CuGaO_2 , and CuAlO_2 led to the formation of CuO and CuM_2O_4 above 673 K, 773 K, 873 K, and 1073 K, respectively. Accordingly, the decomposition of the latter three delafossites is promoted under the conditions of HCl oxidation at a much lower temperature compared with air. The Ellingham diagram further supports the wider region of stability of CuCrO_2 compared to CuAlO_2 (Supporting Information, Figure S1). This demonstrates that the exceptional stability of CuCrO_2 delafossite in HCl oxidation arises from its unprecedented stability under chlorinating and oxidizing atmosphere.

It should be emphasized that a very short period of exposure of any copper phase reported thus far to HCl or HCl and O_2 was sufficient to induce bulk changes and metal loss, leading to catalyst deactivation. For example, the typical

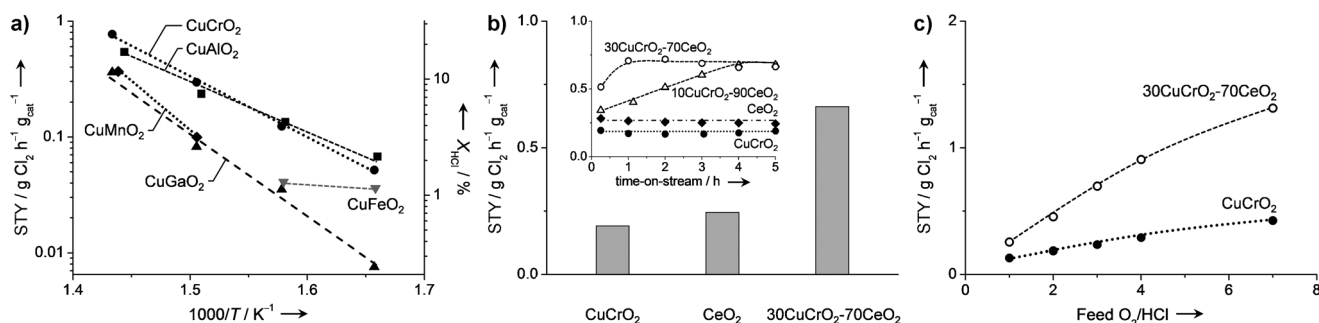


Figure 3. a) Space-time yield (STY) and HCl conversion versus reciprocal temperature for the cuprous delafossites. b) STY of the CuCrO_2 - CeO_2 composites and the constituting pure phases after 5 h of equilibration. Inset: activity of the catalysts over time. c) STY versus feed O_2/HCl ratio for the CuCrO_2 and CuCrO_2 - CeO_2 composite. Conditions: $T_{\text{bed}} = 653 \text{ K}$, $\text{O}_2/\text{HCl} = 2$, $W_{\text{cat}} = 0.5 \text{ g}$, $F_T = 166 \text{ cm}^3 \text{ STP min}^{-1}$, and $P = 1 \text{ bar}$.

CuO/SiO₂ presents signs of bulk chlorination after five minutes of reaction and copper loss of approximately 60% after five hours at 673–723 K. The above delafossites, except the CuCrO₂, also experienced large metal losses. A copper catalyst for Cl₂ production can only be practical if bulk changes do not occur under reaction conditions. After more than seven years of Deacon research in our lab, testing hundreds of catalysts, CuCrO₂ is the first material exhibiting this property. This material is important also because Cr₂O₃ based catalysts deactivate rapidly during HCl oxidation owing to a loss of chromium in the form of volatile Cr⁶⁺ species (CrO₂Cl₂ and CrO₂(OH)₂) generated during reaction.^[12] However, in the delafossite structure, Cr³⁺ is inert towards HCl. Thus, the delafossite structure is crucial to stabilize both copper and chromium, leading to a stable catalytic system in long catalytic runs (see 100 hour test in Figure S2).

The next step was improving the activity of CuCrO₂, which is about one order of magnitude lower than the industrial RuO₂ based catalysts.^[4d] For this purpose, we choose CeO₂, which is an efficient HCl oxidation catalyst^[13] and a catalyst promoter because of its ability to store oxygen.^[14] CuCrO₂-CeO₂ composites were prepared by mechanochemical activation of CuCrO₂ and CeO₂ powders in different proportions. Catalytic data was acquired after five hour tests at O₂/HCl = 2 and T_{bed} = 653 K (Figure 3b). The activity of individual oxides was also included for reference, which showed that both possess similar and low space-time yields (STY). Distinctly, the CuCrO₂-CeO₂ composite with 30 wt % CuCrO₂ shows about four times higher activity compared to either individual phase. This result indicates that CuCrO₂ and CeO₂ show synergy in HCl oxidation. It should be stressed that the grinding process did not alter the total surface area of the composites. The performance of the individual oxides and their porosity did not change upon similar mechanochemical activation. These results rule out a textural origin for the activity enhancement. The composites with 10 wt % and 30 wt % CuCrO₂ exhibited a similar (high) steady-state activity after five hours, demonstrating the wide compositional window in which this effect can be attained (Figure 3b, inset). The inset also shows that the activity increases with time at the beginning of the run, strongly suggesting that the synergistic effect between the delafossite and the ceria phases develops under the reaction conditions. The composite with higher delafossite content reached the steady-state level faster. Further understanding of this effect requires more detailed studies. As expected, the bulk structure as well as the copper content of the catalyst after this test remained unaltered with respect to the fresh sample (Figure S3), thus extending the stability of the individual phases to the composite system at a high degree of HCl conversion. The composites, as exemplified for 30CuCrO₂-70CeO₂, displayed extraordinarily stable Cl₂ production over 200 hours on stream with minimal metal loss (Figure S2). In contrast, the previously reported CuAlO₂ delafossite experienced a 20% copper loss over the same time.^[5]

To understand the mechanism of the synergistic effect of CeO₂ on the activity of CuCrO₂, the influence of feed O₂ content on the activity was investigated (Figure 3c). The activity of the CuCrO₂ was enhanced upon increasing the

oxygen content in the feed and the formal reaction order of O₂ was calculated at approximately 0.5, which suggests that catalyst reoxidation is the limiting step.^[5] This step was remarkably improved in the CuCrO₂-CeO₂ composite as exemplified by two times higher reaction order (0.9) than either single component (Figure 3c).^[13] This result supports that CeO₂ accelerates the catalyst reoxidation step, probably by acting as an oxygen donor/storage material, and thereby boosts the overall HCl oxidation activity in the CuCrO₂-CeO₂ system.

In summary, we discovered the first copper-based material, a CuCrO₂ delafossite, which exhibited a unique resistance to bulk chlorination and, thus, allowed stable Cl₂ production in a long run. Building on this result, we developed a novel CuCrO₂-CeO₂ composite material, which showed a fourfold activity increase compared to its individual components. Thus, a cost-effective chlorine recycling method based on copper catalysts is now a feasible alternative to RuO₂ based systems. Implications of these results for the design of a stable and highly active copper catalyst are also useful for reactions involving an aggressive reaction mixture, such as the oxychlorination of hydrocarbons. In this reaction, as in HCl oxidation, volatilization of copper is a critical issue.

Experimental Section

Cu₂O (Strem, 99.9%), γ-Al₂O₃ (Alfa Aesar, 99.997%), Cr₂O₃ (Strem, 99.995%), Ga₂O₃ (Strem, 99.998%), Mn₂O₃ (Aldrich, 99.999%), and Fe₂O₃ (Strem, 99.999%) were used as precursors. Cuprous delafossites with the formula CuMO₂ (M = Al, Cr, Ga, Fe, Mn) were synthesized by the solid-state reaction of equimolar mixtures of Cu₂O and M₂O₃ homogenized by ball milling for 30 min followed by static-air calcination at 1273–1423 K for 30 h. CuCrO₂ and CuAlO₂ were cooled down in regular air. Pure CuGaO₂, CuFeO₂, and CuMnO₂ required cooling down in a flow of N₂ (details in Table S1). CuCrO₂-CeO₂ composites were prepared by grinding CuCrO₂ and CeO₂ (Aldrich, 34 m² g⁻¹) powders in mass ratios of 10:90 and 30:70 using an agate mortar and pestle for 15 min. The gas-phase oxidation of HCl was studied in a continuous-flow fixed-bed reactor at 1 bar.^[3c] The catalyst (W_{cat} = 0.5 g, particle size = 0.4–0.6 mm) was loaded in the 8 mm inner diameter quartz microreactor and pre-treated in N₂ at 573 K for 30 min. Thereafter, a total flow (F_T) of 166 cm³ STP min⁻¹ containing 10 vol % HCl and 0–70 vol % O₂ balanced with N₂ was fed into the reactor at bed temperatures (T_{bed}) in the range of 573–690 K. Cl₂ was quantified by iodometric titration using a Mettler Toledo G20 Compact Titrator. The percentage of HCl conversion was determined as X_{HCl} = (2 mole Cl₂ at the reactor outlet/1 mole HCl at the reactor inlet) × 100 and the space-time yield as STY = grams of Cl₂/(hour × gram of catalyst). The used catalysts were collected after rapid quenching of the reactor to room temperature in N₂ flow and characterized by X-ray diffraction (PANalytical X'Pert PRO-MPD) and inductively coupled plasma-optical emission spectroscopy (Horiba Jobin Yvon Ultima 2).

Received: May 17, 2013

Published online: June 20, 2013

Keywords: cerium oxide · chlorine production · CuCrO₂ · delafossite · heterogeneous catalysis

- [1] J. Pérez-Ramírez, C. Mondelli, T. Schmidt, O. F. K. Schlüter, A. Wolf, L. Mleczko, T. Dreier, *Energy Environ. Sci.* **2011**, *4*, 4786–4799.
- [2] H. Deacon (Gaskell, Deacon and Co.), US85370, **1868**. Between 1868 and 1876, Henry Deacon filed more than 15 patents based on copper salts and oxides, which were impregnated on porous carriers (burnt clay, cinders, magnesia, pumice) and promoted by sulfate of sodium or potash.
- [3] a) C. W. Davis, F. A. Ehlers, R. G. Ellis, W. Creek (The Dow Chemical Company), US2547928, **1951**; b) W. F. Engel, F. Wattimena (Shell Oil Company), US3210158, **1965**; c) F. Wattimena, W. M. H. Sachtler, *Stud. Surf. Sci. Catal.* **1981**, *7*, 816–827; d) M. Mortensen, R. G. Minet, T. T. Tsotsis, S. Benson, *Chem. Eng. Sci.* **1999**, *54*, 2131–2139; e) A. P. Amrute, C. Mondelli, M. A. G. Hevia, J. Pérez-Ramírez, *J. Phys. Chem. C* **2011**, *115*, 1056–1063.
- [4] a) D. Crihan, M. Knapp, S. Zweidinger, E. Lundgren, C. J. Weststrate, J. N. Andersen, A. P. Seitsonen, H. Over, *Angew. Chem.* **2008**, *120*, 2161–2164; *Angew. Chem. Int. Ed.* **2008**, *47*, 2131–2134; b) N. López, J. Gomez-Segura, R. P. Marín, J. Pérez-Ramírez, *J. Catal.* **2008**, *255*, 29–39; c) K. Seki, *Catal. Surv. Asia* **2010**, *14*, 168–175; d) C. Mondelli, A. P. Amrute, F. Krumeich, T. Schmidt, J. Pérez-Ramírez, *ChemCatChem* **2011**, *3*, 657–660; e) D. Teschner, R. Farra, L. Yao, R. Schlögl, H. Soerijanto, R. Schomaecker, T. Schmidt, L. Szentmiklósi, A. P. Amrute, C. Mondelli, J. Pérez-Ramírez, G. Novell-Leruth, N. López, *J. Catal.* **2012**, *285*, 273–284; f) A. P. Amrute, C. Mondelli, T. Schmidt, R. Hauert, J. Pérez-Ramírez, *ChemCatChem* **2013**, *5*, 748–756.
- [5] C. Mondelli, A. P. Amrute, T. Schmidt, J. Pérez-Ramírez, *Chem. Commun.* **2011**, *47*, 7173–7175.
- [6] C. T. Prewitt, R. D. Shannon, D. B. Rogers, *Inorg. Chem.* **1971**, *10*, 719–723.
- [7] A. Buljan, P. Alemany, E. Ruiz, *J. Phys. Chem. B* **1999**, *103*, 8060–8066.
- [8] a) H. Kawazoe, M. Yasukawa, H. Hyodo, M. Kurita, H. Yanagi, H. Hosono, *Nature* **1997**, *389*, 939–942; b) R. Bywalez, S. Götzendörfer, P. Löbmann, *J. Mater. Chem.* **2010**, *20*, 6562–6570; c) D. O. Scanlon, G. W. Watson, *J. Mater. Chem.* **2011**, *21*, 3655–3663.
- [9] a) J. R. Monnier, M. J. Hanrahan, G. Apai, *J. Catal.* **1985**, *92*, 119–126; b) J. Christopher, C. S. Swamy, *J. Mater. Sci.* **1992**, *27*, 1353–1356; c) S. Saadi, A. Bouguelia, M. Trari, *Solar Energy* **2006**, *80*, 272–280; d) S. Kameoka, M. Okada, A. P. Tsai, *Catal. Lett.* **2008**, *120*, 252–256; e) W. Ketir, A. Bouguelia, M. Trari, *Desalination* **2009**, *244*, 144–152.
- [10] a) W. Dannhauser, P. A. Vaughan, *J. Am. Chem. Soc.* **1955**, *77*, 896–897; b) B. U. Köhler, M. Jansen, *Z. Anorg. Allg. Chem.* **1986**, *543*, 73–80.
- [11] F. Damay, M. Poienar, C. Martin, A. Maignan, J. Rodriguez-Carvajal, G. André, J. P. Doumerc, *Phys. Rev. B* **2009**, *80*, 094410.
- [12] A. P. Amrute, C. Mondelli, J. Pérez-Ramírez, *Catal. Sci. Technol.* **2012**, *2*, 2057–2065.
- [13] a) A. P. Amrute, C. Mondelli, M. Moser, G. Novell-Leruth, N. López, D. Rosenthal, R. Farra, M. E. Schuster, D. Teschner, T. Schmidt, J. Pérez-Ramírez, *J. Catal.* **2012**, *286*, 287–297; b) M. Moser, C. Mondelli, T. Schmidt, F. Girgsdies, M. E. Schuster, R. Farra, L. Szentmiklosi, D. Teschner, J. Pérez-Ramírez, *Appl. Catal. B* **2013**, *132–133*, 123–131.
- [14] G. Kim, *Ind. Eng. Chem. Prod. Res. Dev.* **1982**, *21*, 267–274.